Electronic Supplementary Information (ESI) for Dalton Transactions This journal is © The Royal Society of Chemistry 2018

Supporting Information For

A new 3D luminescent Zn(II)-organic framework containing quinoline-2,6-dicarboxylate linker for the highly selective sensing of Fe(III) ion

Chiranjib Gogoi,[a] *Muhammed Yousufuddin*[b] *and Shyam Biswas**[a]

[a] Department of Chemistry, Indian Institute of Technology Guwahati, 781039, Assam, India.

[b] Life and Health Sciences Department, The University of North Texas at Dallas, Dallas, Texas 75241, United States.

* To whom correspondence should be addressed. E-mail: sbiswas@iitg.ernet.in; Tel: 91-3612583309.

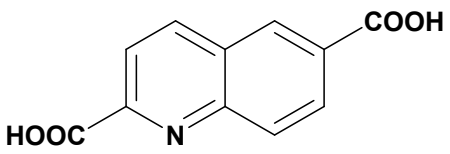

Figure S1. Ligand used for the present work.

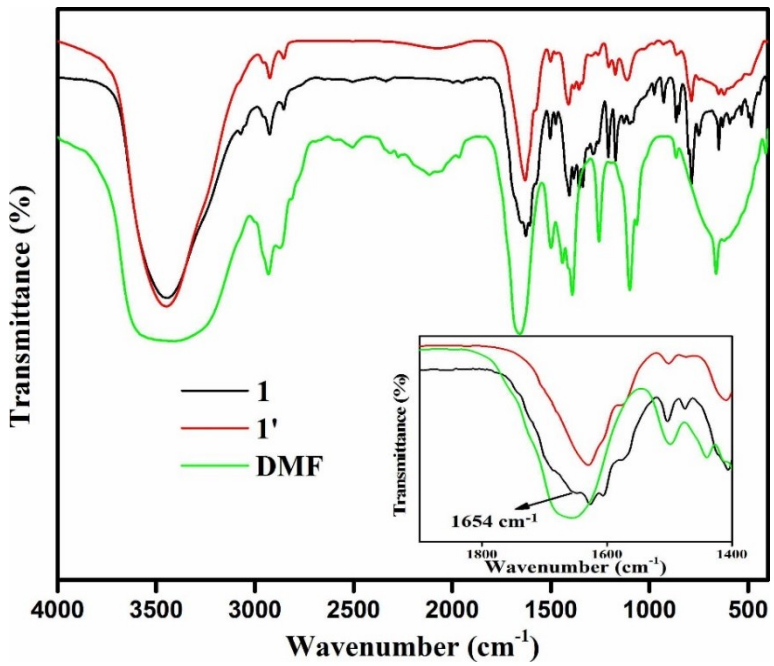

Figure S2. FT-IR spectra of compound **1** (black), **1'** (red) and DMF (green).

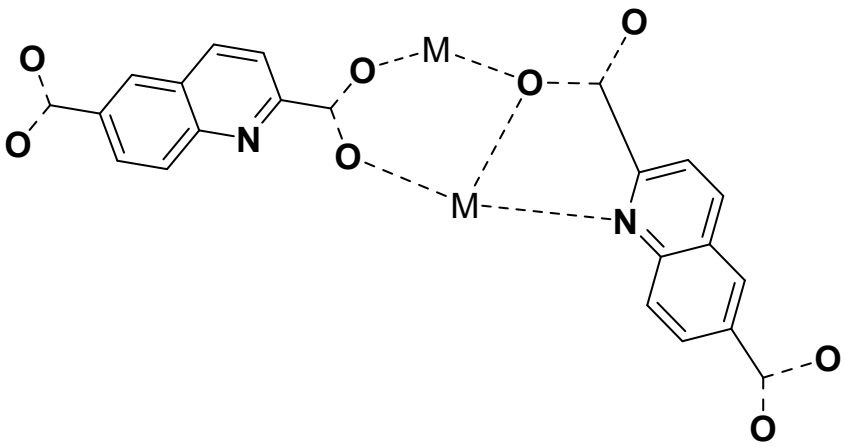

Scheme S1. Coordination and *bis*-chelation mode displayed by QDA ligand in compound **1**.

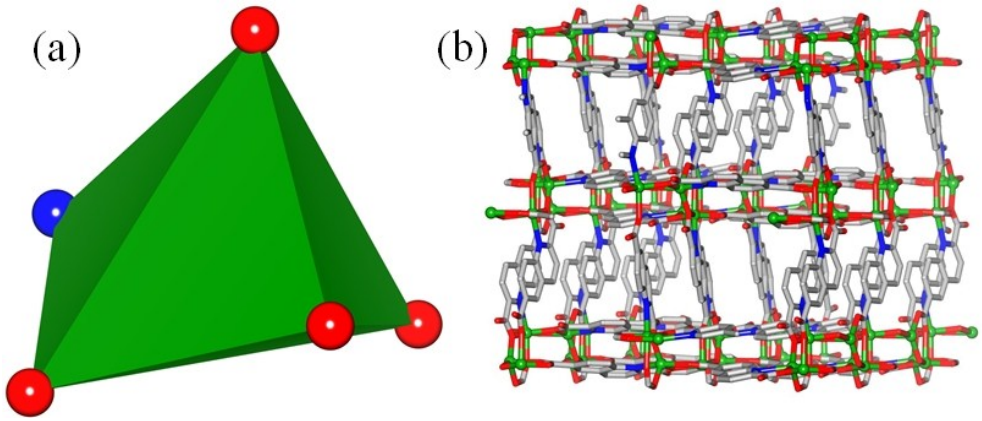

Figure S3. (a) Metal-organic square pyramidal polyhedra found within compound **1** constructed via coordination of QDA ligands with Zn^{2+} ions. (b) Side view of the overall 3D framework of compound **1**.

Table S1. Single-crystal X-ray data and structure refinement parameters for compound **1**.

Formula	$C_{11}H_5NO_4Zn$
Formula Weight	280.53
Crystal System	Tetragonal
Space group	$I4_1/a$
a/Å	19.9088(3)
b/Å	19.9088(3)
c/Å	12.1905(3)
V/Å^3	4831.83(19)
Z	16
D_e/g cm^{-3}	1.543
μ Mo K_α/mm^{-1}	2.033
F000	2240.0
T/K	293(2)
Theta range	2.894 to 28.697°
Total no. of reflections	5395
Independent reflections	2747 [R(int) = 0.0174]
Observed reflections	1830
Parameters refined	154
Final R indices [I>2sigma(I)]	R_1 = 0.0274, wR_2 = 0.0671
R indices (all data)	R_1 = 0.0378, wR_2 = 0.0723

GOF (F^2)	1.049
Crystal Size	0.26 × 0.24 × 0.22 mm^3
Index ranges	-26<=*h*<=13, -21<=*k*<=25, -16<=*l*<=8
Absorption correction	Semi-empirical from equivalents
Max. and min. transmission	0.639 and 0.595
Refinement method	Full-matrix least-squares on F^2
Data / restraints / parameters	2747 / 0 / 154
Extinction coefficient	n/a
Largest diff. peak and hole	0.379 and -0.207 e.$Å^{-3}$

Table S2. Atomic coordinates (x 10^4) and equivalent isotropic displacement parameters ($Å^2$x 10^3) for compound **1**. U(eq) is defined as one third of the trace of the orthogonalized U^{ij} tensor.

Zn(1)	7017(1)	449(1)	1674(1)	28(1)
O(13)	6705(1)	4077(1)	9034(1)	50(1)
O(14)	6899(1)	4606(1)	7464(1)	32(1)
O(16)	7059(1)	550(1)	4253(1)	52(1)
O(17)	6993(1)	1190(1)	2745(1)	45(1)
C(2)	6773(1)	3427(1)	7404(2)	35(1)
C(3)	6628(1)	2822(1)	7940(2)	51(1)
C(4)	6632(2)	2242(1)	7344(2)	55(1)
C(5)	6783(1)	2265(1)	6215(2)	40(1)
C(6)	6822(1)	1678(1)	5562(2)	46(1)
C(7)	6968(1)	1723(1)	4465(2)	38(1)
C(8)	7066(1)	2359(1)	3987(2)	45(1)
C(9)	7048(1)	2929(1)	4597(2)	42(1)
C(10)	6912(1)	2898(1)	5731(2)	34(1)
N(11)	6904(1)	3474(1)	6339(1)	31(1)
C(12)	6785(1)	4075(1)	8043(2)	35(1)
C(15)	7016(1)	1097(1)	3773(2)	39(1)

Table S3. Bond lengths [Å] and angles [°] for compound **1**.

Zn(1)-O(17)	1.9708(15)
Zn(1)-O(14)#1	1.9941(14)
Zn(1)-O(14)#2	2.0266(15)
Zn(1)-O(16)#3	2.0599(15)
Zn(1)-N(11)#2	2.1875(17)
O(13)-C(12)	1.218(3)
O(14)-C(12)	1.293(3)
O(16)-C(15)	1.239(3)
O(17)-C(15)	1.268(3)
C(2)-N(11)	1.327(3)
C(2)-C(3)	1.400(3)
C(2)-C(12)	1.507(3)
C(3)-C(4)	1.365(3)
C(3)-H(3)	0.9300
C(4)-C(5)	1.409(3)
C(4)-H(4)	0.9300
C(5)-C(10)	1.415(3)
C(5)-C(6)	1.416(3)
C(6)-C(7)	1.372(3)
C(6)-H(6)	0.9300
C(7)-C(8)	1.408(3)
C(7)-C(15)	1.508(3)
C(8)-C(9)	1.356(3)
C(8)-H(8)	0.9300
C(9)-C(10)	1.410(3)
C(9)-H(9)	0.9300
C(10)-N(11)	1.367(3)
O(17)-Zn(1)-O(14)#1	106.11(7)
O(17)-Zn(1)-O(14)#2	122.89(6)
O(14)#1-Zn(1)-O(14)#2	130.95(7)
O(17)-Zn(1)-O(16)#3	89.95(7)
O(14)#1-Zn(1)-O(16)#3	94.94(7)
O(14)#2-Zn(1)-O(16)#3	87.69(6)
O(17)-Zn(1)-N(11)#2	93.79(7)
O(14)#1-Zn(1)-N(11)#2	98.72(6)

O(14)#2-Zn(1)-N(11)#2	77.41(6)
O(16)#3-Zn(1)-N(11)#2	164.22(7)
C(12)-O(14)-Zn(1)#4	114.92(13)
C(12)-O(14)-Zn(1)#5	119.50(13)
Zn(1)#4-O(14)-Zn(1)#5	125.16(7)
C(15)-O(16)-Zn(1)#6	148.75(17)
C(15)-O(17)-Zn(1)	123.03(15)
N(11)-C(2)-C(3)	123.9(2)
N(11)-C(2)-C(12)	116.22(18)
C(3)-C(2)-C(12)	119.9(2)
C(4)-C(3)-C(2)	118.6(2)
C(4)-C(3)-H(3)	120.7
C(2)-C(3)-H(3)	120.7
C(3)-C(4)-C(5)	119.6(2)
C(3)-C(4)-H(4)	120.2
C(5)-C(4)-H(4)	120.2
C(4)-C(5)-C(10)	118.4(2)
C(4)-C(5)-C(6)	122.2(2)
C(10)-C(5)-C(6)	119.4(2)
C(7)-C(6)-C(5)	120.4(2)
C(7)-C(6)-H(6)	119.8
C(5)-C(6)-H(6)	119.8
C(6)-C(7)-C(8)	119.5(2)
C(6)-C(7)-C(15)	120.4(2)
C(8)-C(7)-C(15)	120.2(2)
C(9)-C(8)-C(7)	121.4(2)
C(9)-C(8)-H(8)	119.3
C(7)-C(8)-H(8)	119.3
C(8)-C(9)-C(10)	120.4(2)
C(8)-C(9)-H(9)	119.8
C(10)-C(9)-H(9)	119.8
N(11)-C(10)-C(9)	119.9(2)
N(11)-C(10)-C(5)	121.27(19)
C(9)-C(10)-C(5)	118.9(2)
C(2)-N(11)-C(10)	118.28(18)
C(2)-N(11)-Zn(1)#5	111.91(14)
C(10)-N(11)-Zn(1)#5	129.80(14)
O(13)-C(12)-O(14)	124.2(2)

O(13)-C(12)-C(2)	120.9(2)
O(14)-C(12)-C(2)	114.91(19)
O(16)-C(15)-O(17)	126.7(2)
O(16)-C(15)-C(7)	117.8(2)
O(17)-C(15)-C(7)	115.5(2)

Symmetry transformations used to generate equivalent atoms:

#1 x,y-1/2,-z+1 #2 y+1/4,-x+3/4,-z+3/4 #3 y+3/4,-x+3/4,z-1/4

#4 x,y+1/2,-z+1 #5 -y+3/4,x-1/4,-z+3/4 #6 -y+3/4,x-3/4,z+1/4

Table S4. Anisotropic displacement parameters ($Å^2 x\ 10^3$) for compound **1**. The anisotropic displacement factor exponent takes the form: $-2\pi^2[\ h^2\ a^{*2} U^{11} + ...\ + 2\ h\ k\ a^*\ b^*\ U^{12}\ ]$

	U^{11}	U^{22}	U^{33}	U^{23}	U^{13}	U^{12}
Zn(1)	29(1)	29(1)	26(1)	2(1)	0(1)	-1(1)
O(13)	72(1)	47(1)	31(1)	-3(1)	10(1)	-2(1)
O(14)	40(1)	27(1)	29(1)	-2(1)	5(1)	-2(1)
O(16)	88(1)	26(1)	43(1)	-3(1)	-11(1)	2(1)
O(17)	63(1)	35(1)	37(1)	-9(1)	-2(1)	0(1)
C(2)	41(1)	32(1)	32(1)	0(1)	5(1)	-4(1)
C(3)	81(2)	41(1)	31(1)	2(1)	11(1)	-10(1)
C(4)	89(2)	33(1)	42(1)	6(1)	8(1)	-8(1)
C(5)	57(2)	31(1)	34(1)	2(1)	2(1)	-4(1)
C(6)	67(2)	29(1)	42(1)	0(1)	-3(1)	-4(1)
C(7)	46(1)	31(1)	37(1)	-3(1)	-2(1)	1(1)
C(8)	67(2)	35(1)	35(1)	-5(1)	11(1)	-5(1)
C(9)	63(2)	28(1)	36(1)	1(1)	10(1)	-5(1)
C(10)	38(1)	29(1)	34(1)	0(1)	2(1)	-2(1)
N(11)	37(1)	27(1)	30(1)	0(1)	3(1)	-3(1)
C(12)	35(1)	36(1)	34(1)	-2(1)	5(1)	1(1)
C(15)	43(1)	32(1)	41(1)	-7(1)	-3(1)	-2(1)

Table S5. Hydrogen coordinates (x 10^4) and isotropic displacement parameters (Å^{2}x 10^3) for compound **1**.

	x	y	z	U(eq)
H(3)	6531	2816	8686	61
H(4)	6536	1834	7680	66
H(6)	6748	1260	5879	55
H(8)	7147	2390	3237	55
H(9)	7124	3342	4265	51

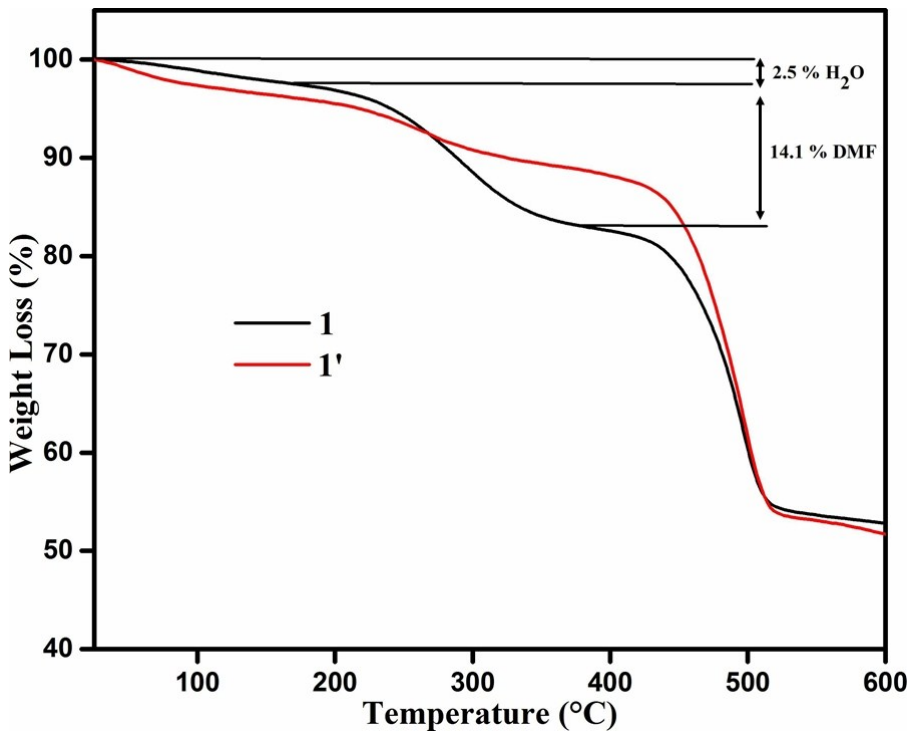

Figure S4. TG curves of **1** and **1'** recorded in an argon atmosphere in the temperature range of 25-600 °C with a heating rate of 10 °C/min.

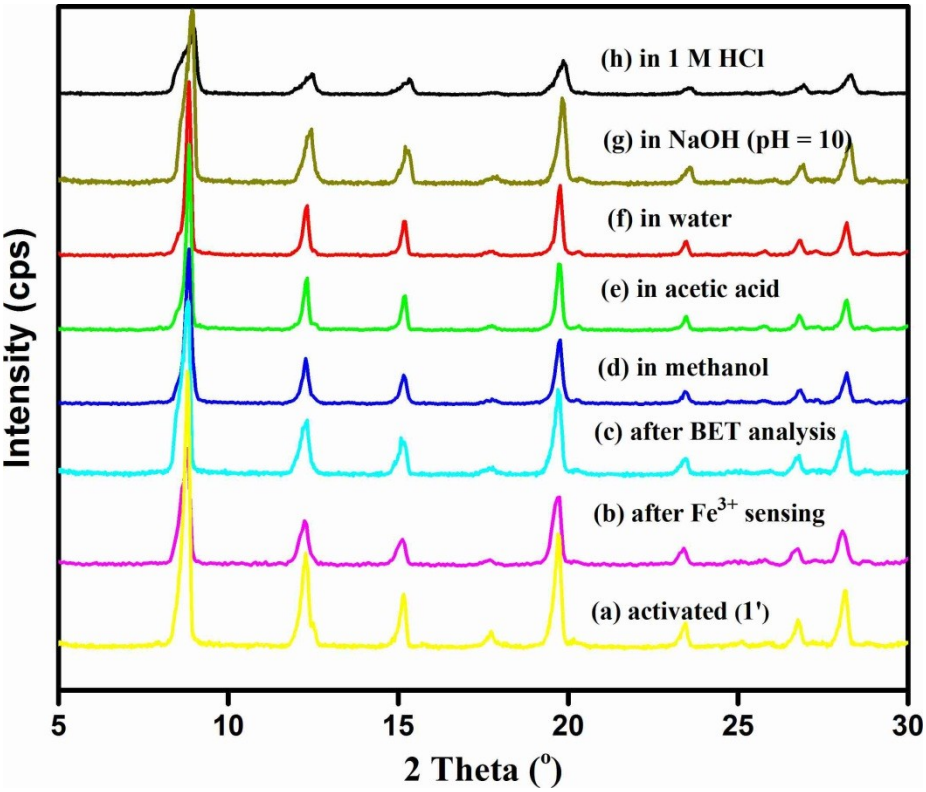

Figure S5. XRPD patterns of compound **1** in different forms: (a) activated, (b) after 5 cycles of fluorescence titration experiments with Fe^{3+} solution, (c) after BET analysis, (d) after treatment with methanol, (e) after treatment with acetic acid, (f) after treatment with water, (g) after treatment with NaOH solution (pH = 10), and (h) after treatment with 1(M) HCl.

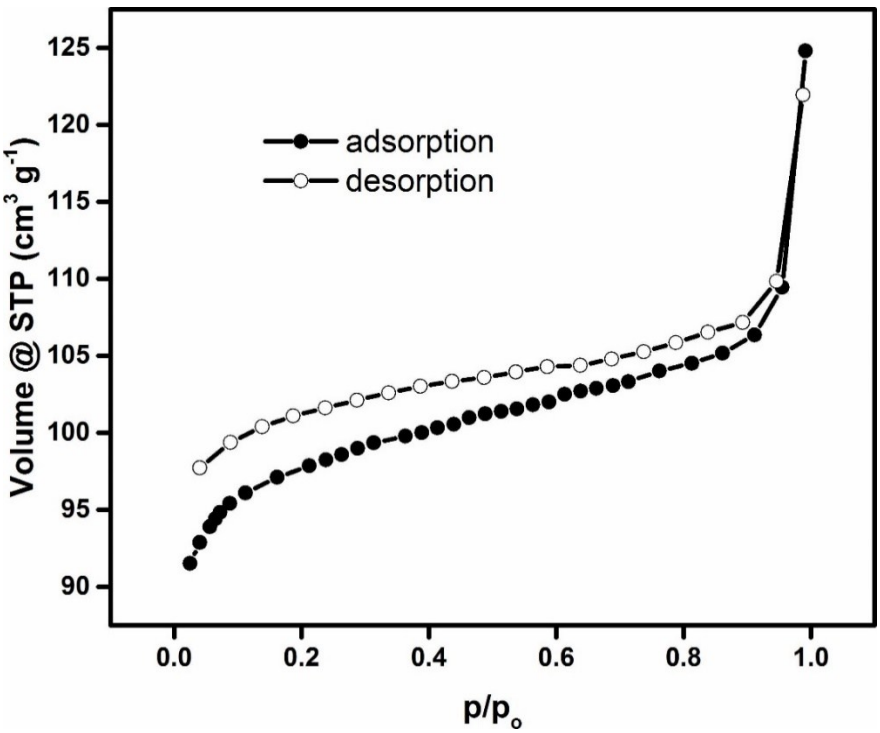

Figure S6. N_2 adsorption (filled circles) and desorption (empty circles) isotherms of thermally activated **1'** measured at –196 °C.

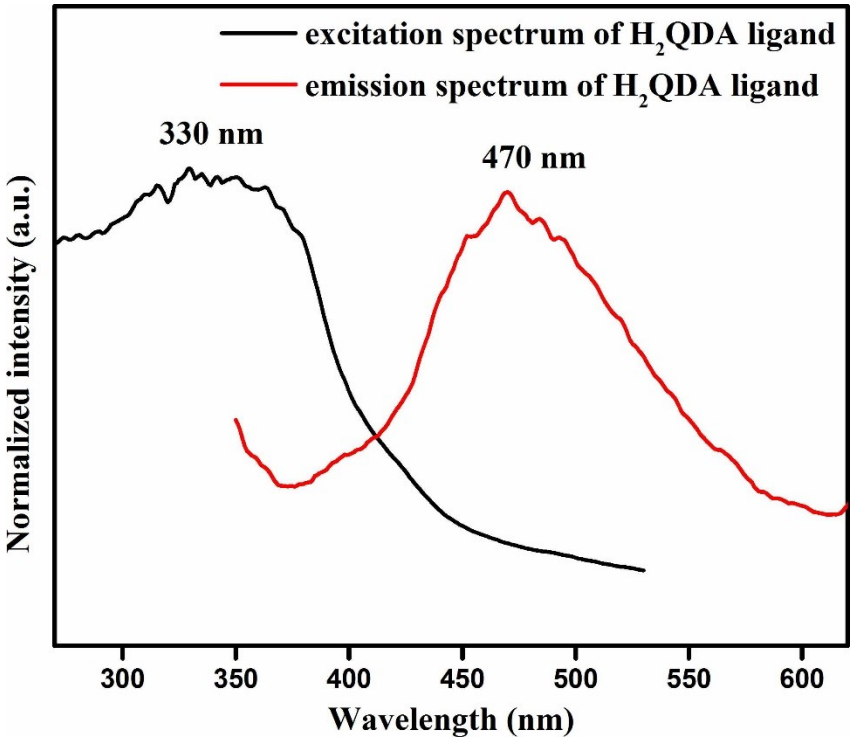

Figure S7. Fluorescence excitation and emission spectra of H_2QDA ligand in the solid state.

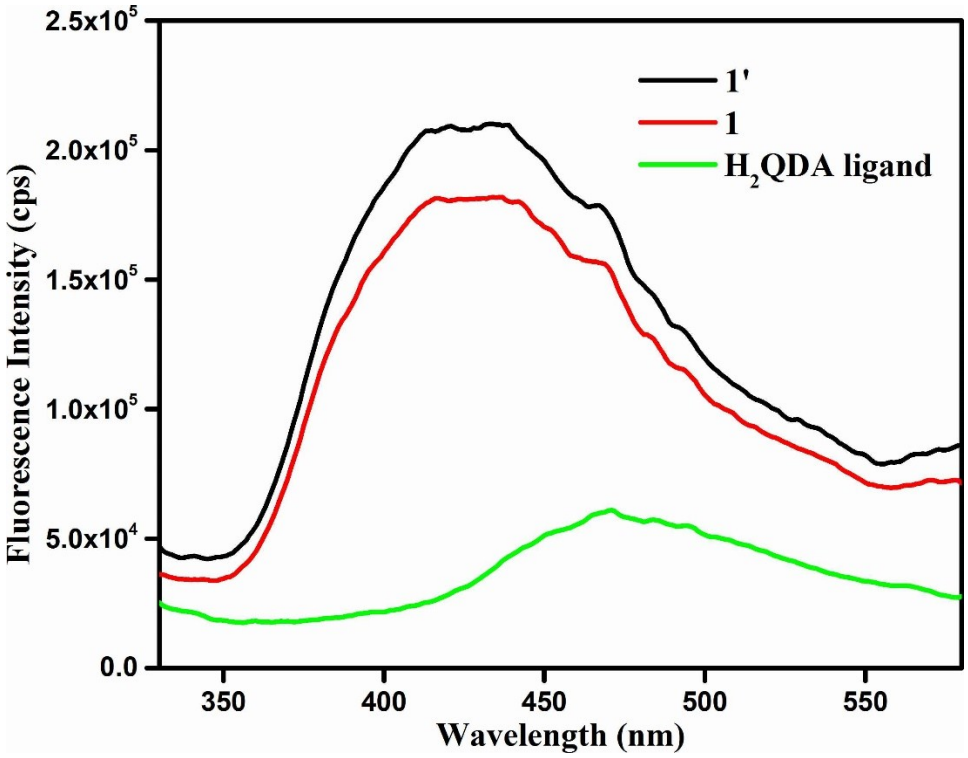

Figure S8. Fluorescence emission spectra of **1**, **1'** and H_2QDA ligand in the solid state (λ_{ex} = 310 nm).

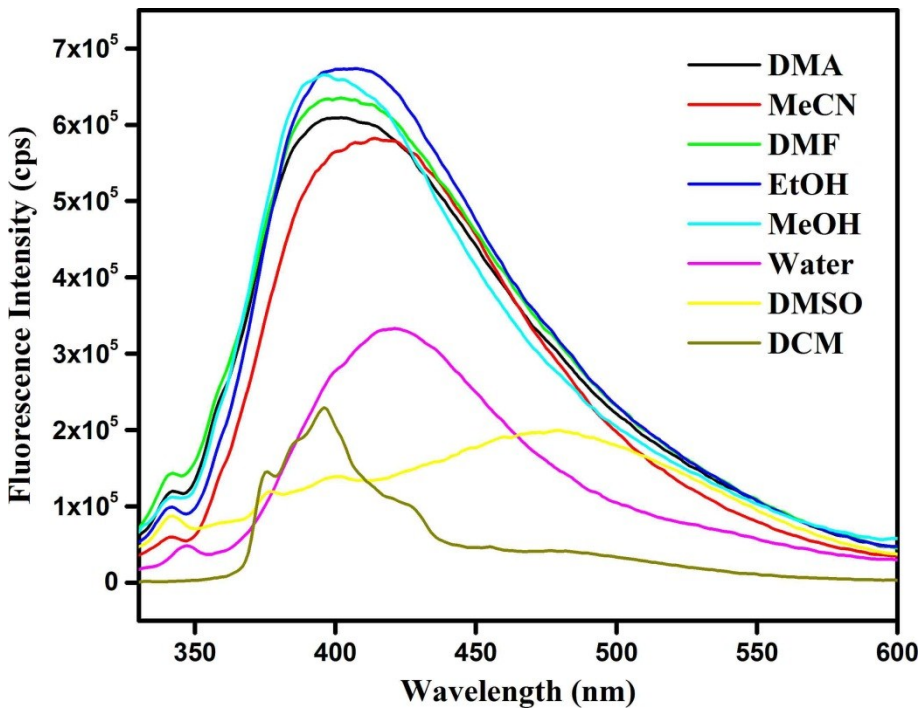

Figure S9. Fluorescence emission spectra of **1'** in common organic solvents (λ_{ex} = 310 nm).

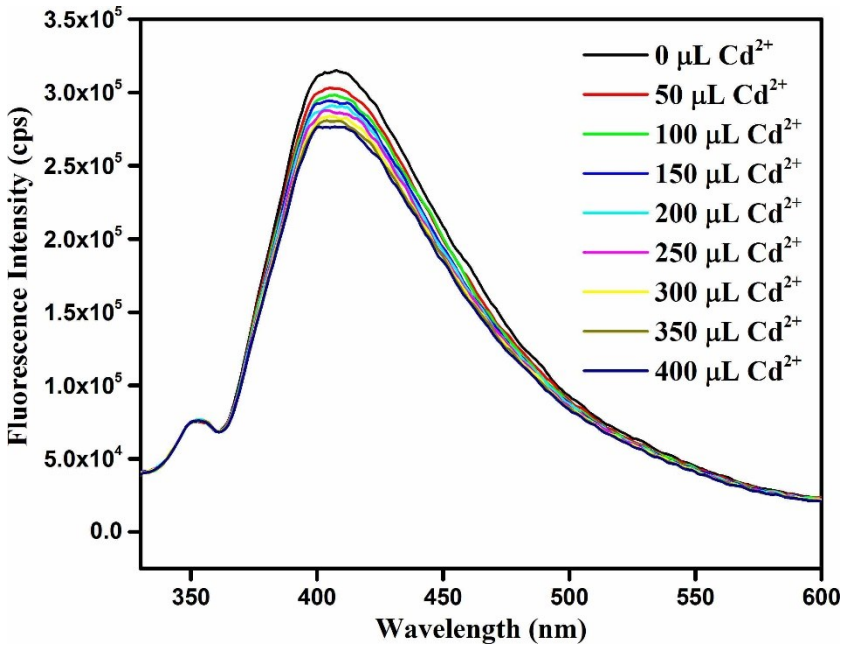

Figure S10. Change in the fluorescence intensity of **1′** upon incremental addition of 10 mM Cd^{2+} solution.

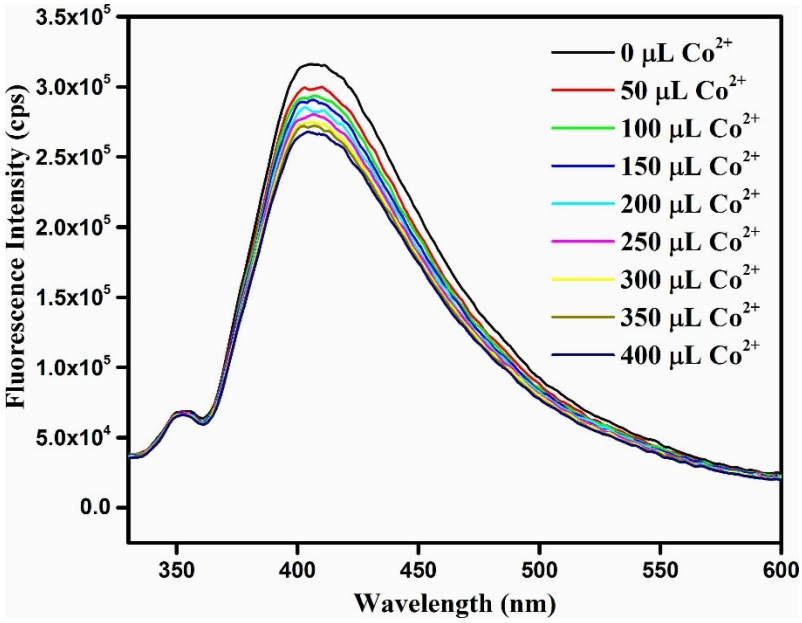

Figure S11. Change in the fluorescence intensity of **1′** upon incremental addition of 10 mM Co^{2+} solution.

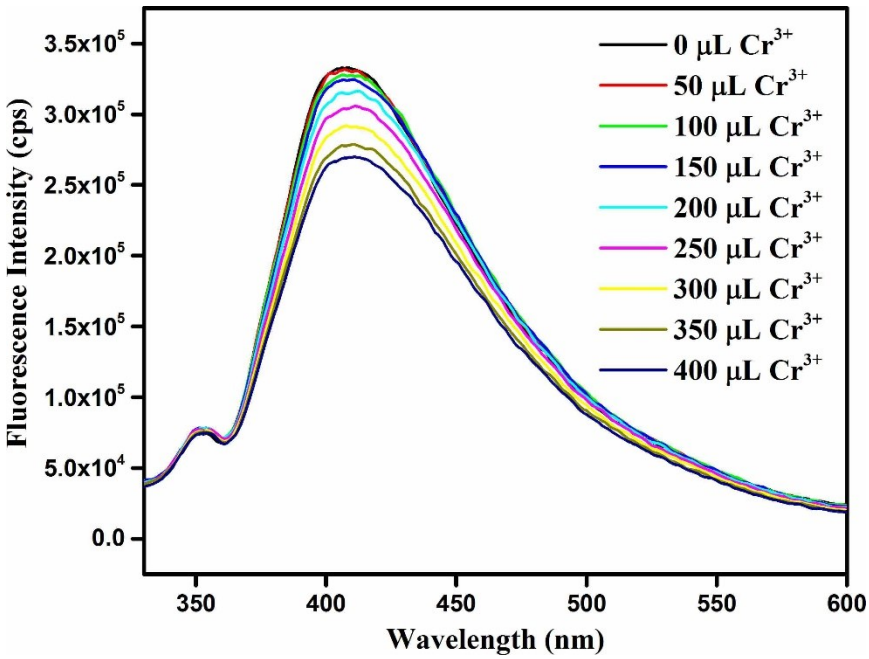

Figure S12. Change in the fluorescence intensity of **1′** upon incremental addition of 10 mM Cr^{3+} solution.

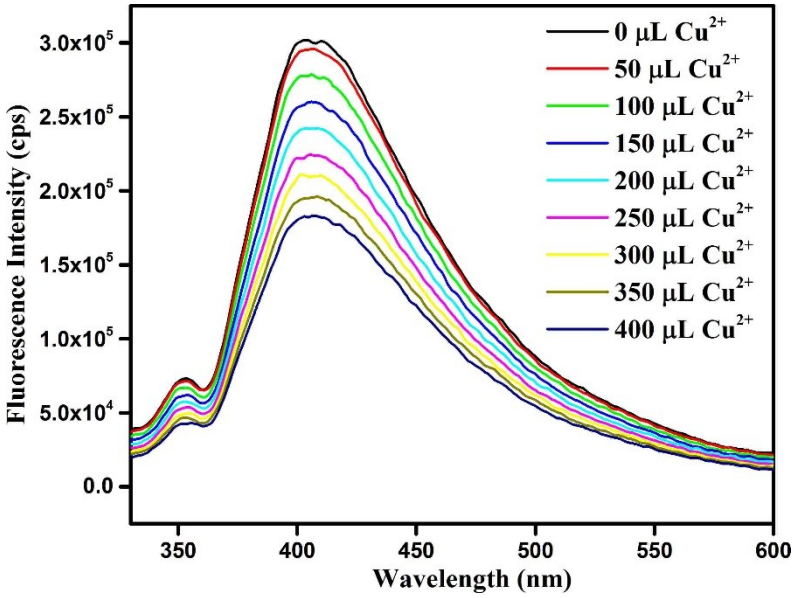

Figure S13. Change in the fluorescence intensity of **1′** upon incremental addition of 10 mM Cu^{2+} solution.

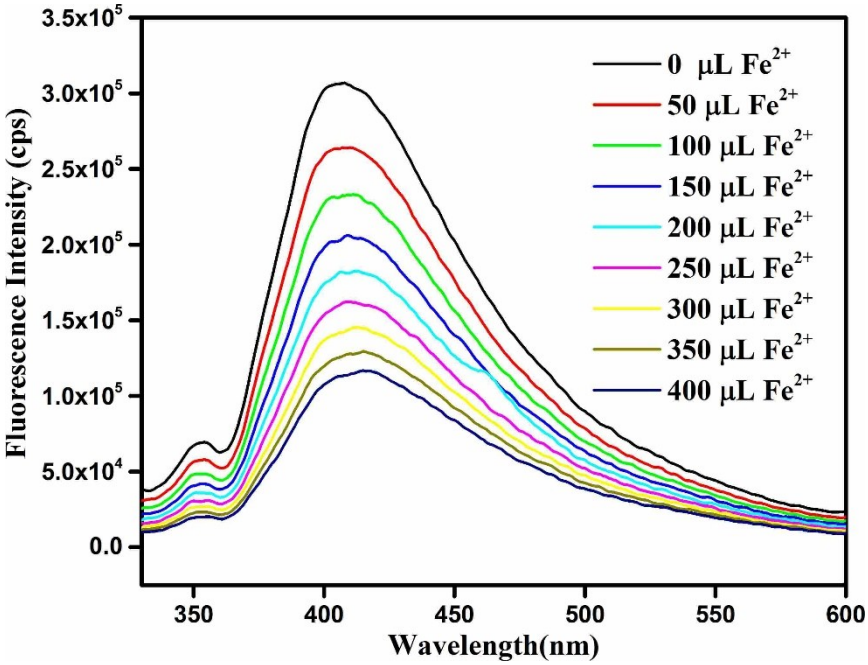

Figure S14. Change in the fluorescence intensity of **1′** upon incremental addition of 10 mM Fe^{2+} solution.

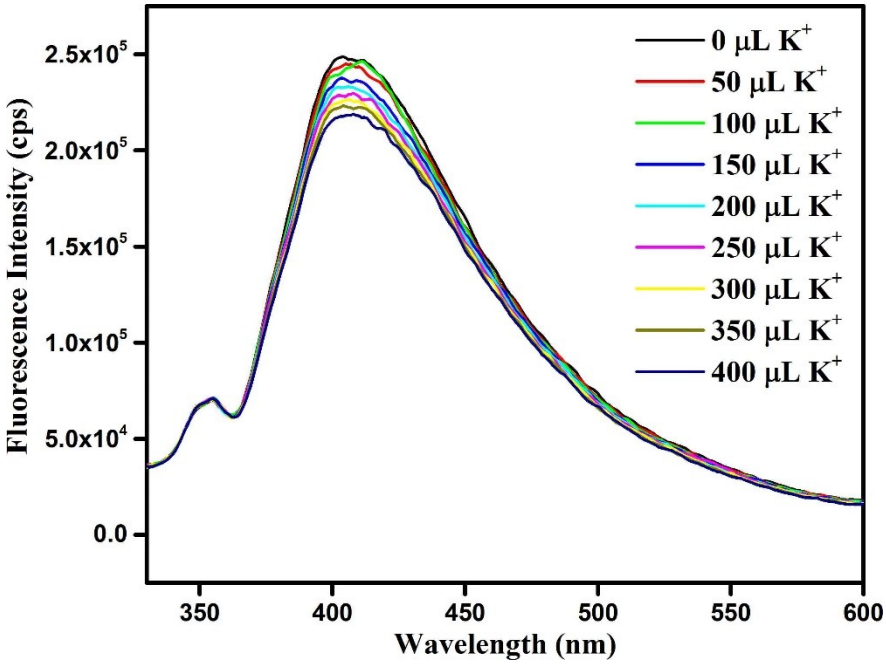

Figure S15. Change in the fluorescence intensity of **1′** upon incremental addition of 10 mM K^+ solution.

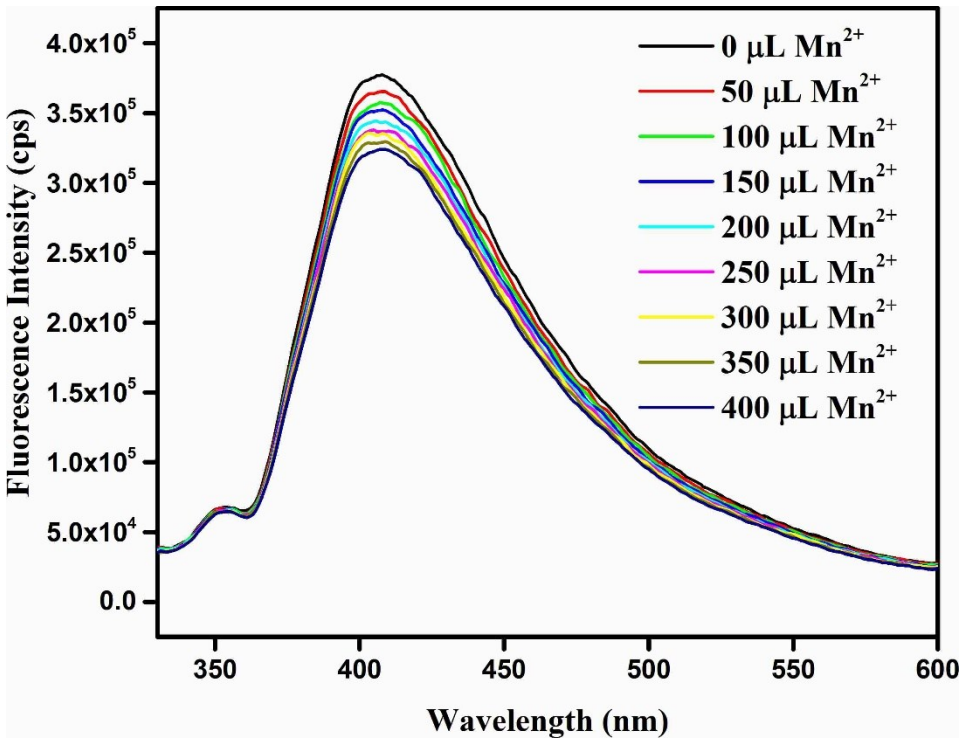

Figure S16. Change in the fluorescence intensity of **1′** upon incremental addition of 10 mM Mn^{2+} solution.

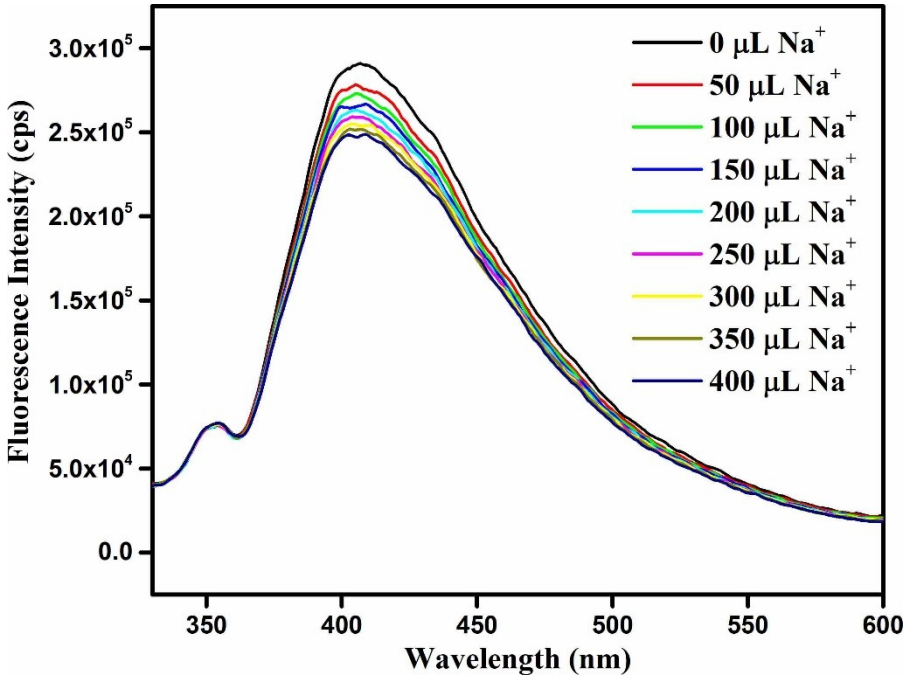

Figure S17. Change in the fluorescence intensity of **1′** upon incremental addition of 10 mM Na^+ solution.

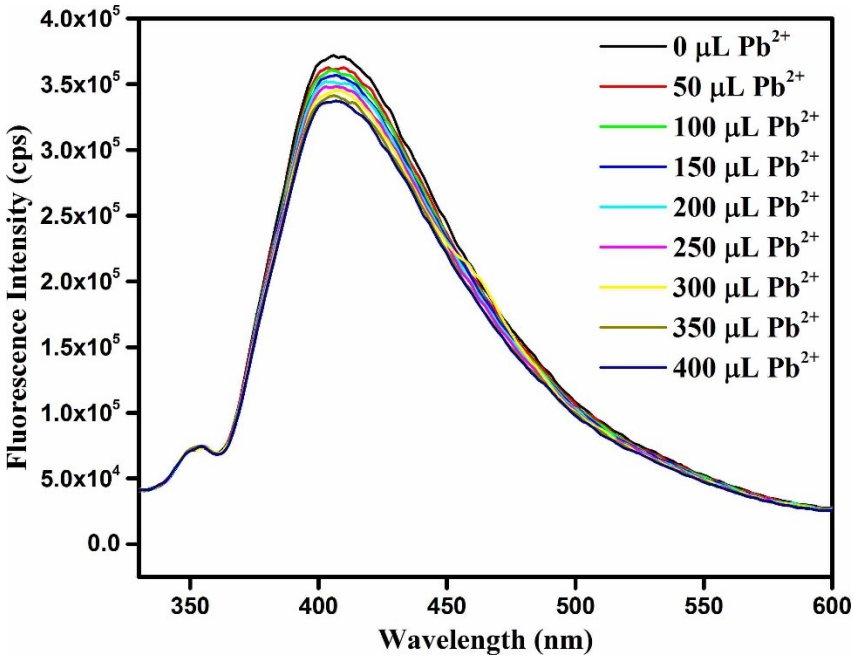

Figure S18. Change in the fluorescence intensity of **1′** upon incremental addition of 10 mM Pb^{2+} solution.

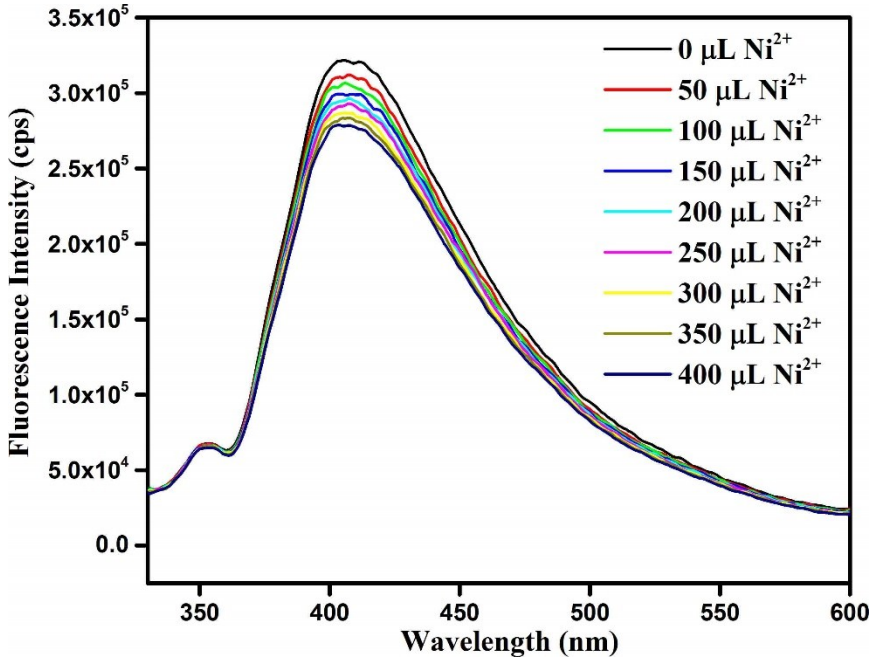

Figure S19. Change in the fluorescence intensity of **1′** upon incremental addition of 10 mM Ni^{2+} solution.

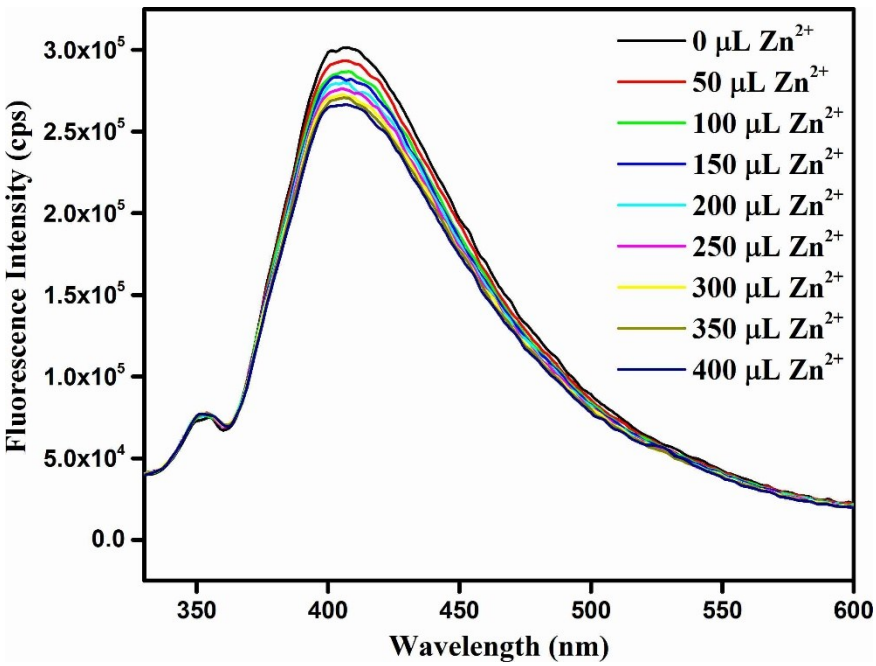

Figure S20. Change in the fluorescence intensity of **1′** upon incremental addition of 10 mM Zn^{2+} solution.

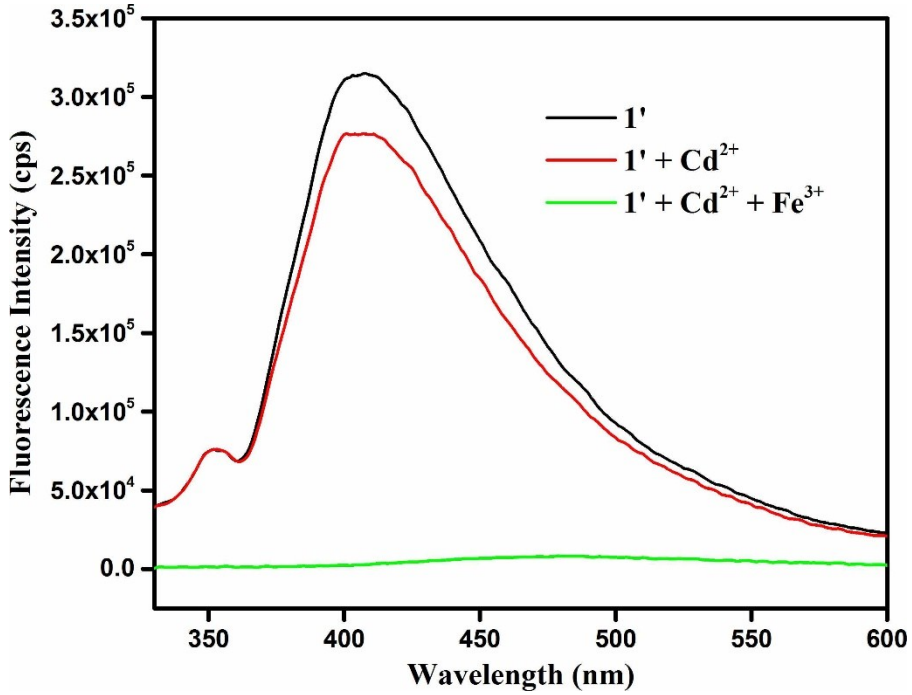

Figure S21. Change in the fluorescence intensity of **1′** upon addition of 10 mM Cd^{2+} solution (400 μL) in presence of 10 mM Fe^{3+} (400 μL) solution.

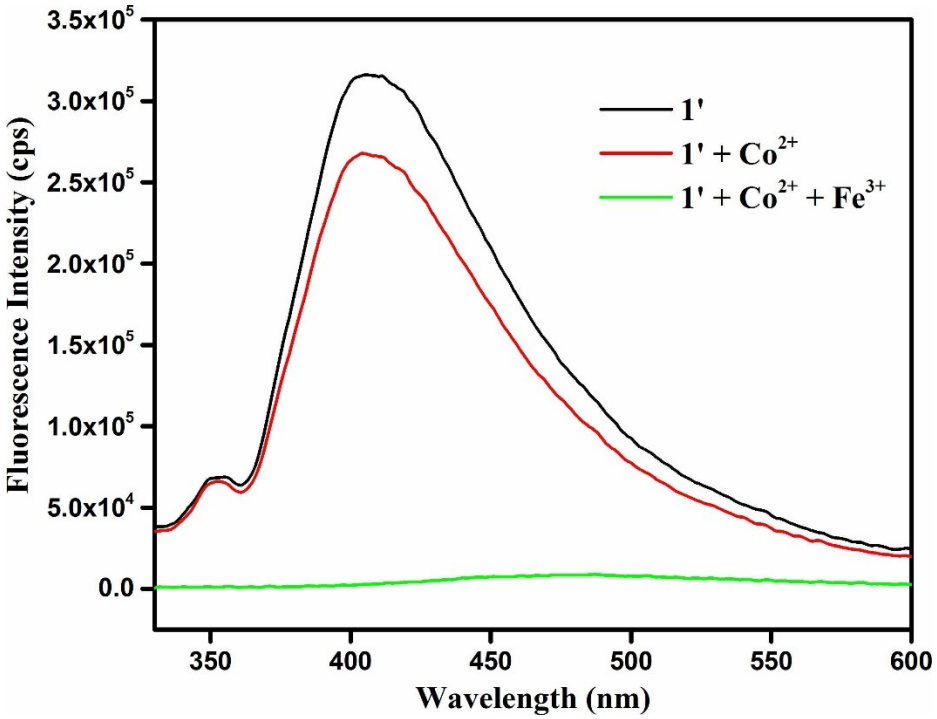

Figure S22. Change in the fluorescence intensity of **1′** upon addition of 10 mM Co^{2+} solution (400 μL) in presence of 10 mM Fe^{3+} (400 μL) solution.

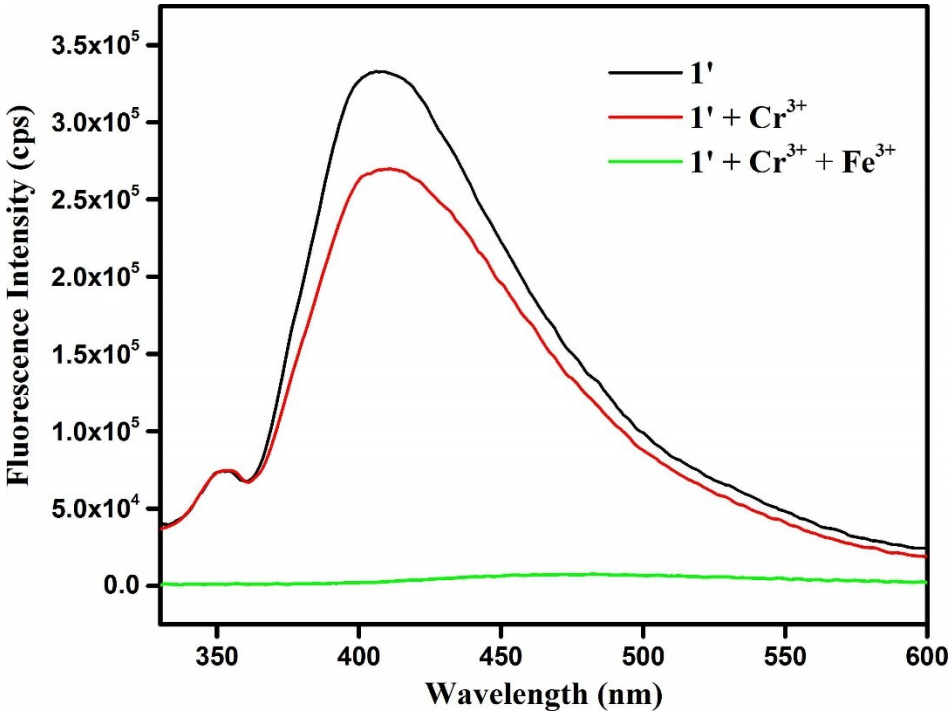

Figure S23. Change in the fluorescence intensity of **1′** upon addition of 10 mM Cr^{3+} solution (400 μL) in presence of 10 mM Fe^{3+} (400 μL) solution.

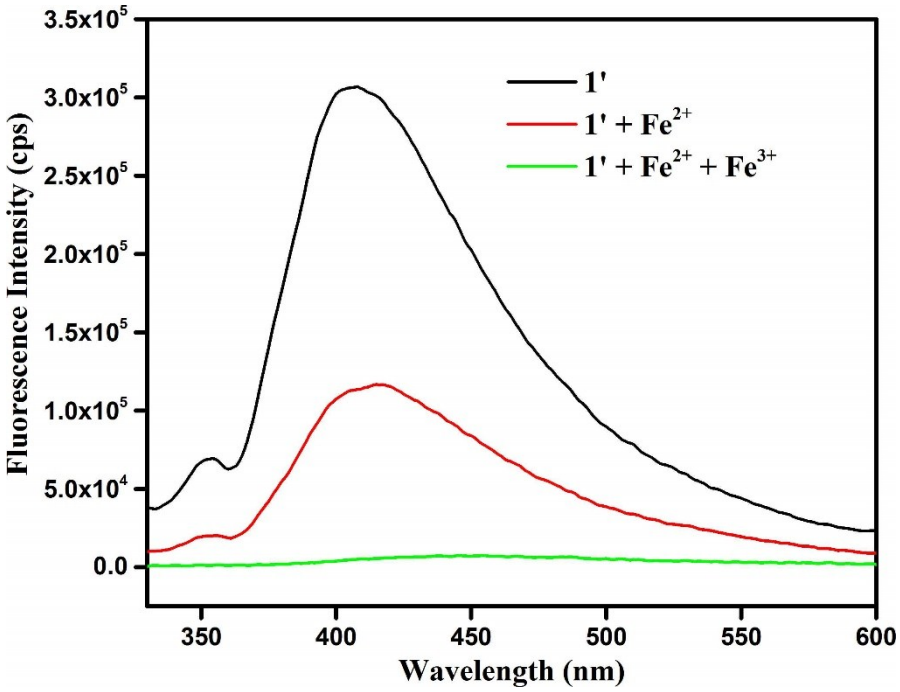

Figure S24. Change in the fluorescence intensity of **1′** upon addition of 10 mM Fe^{2+} solution (400 μL) in presence of 10 mM Fe^{3+} (400 μL) solution.

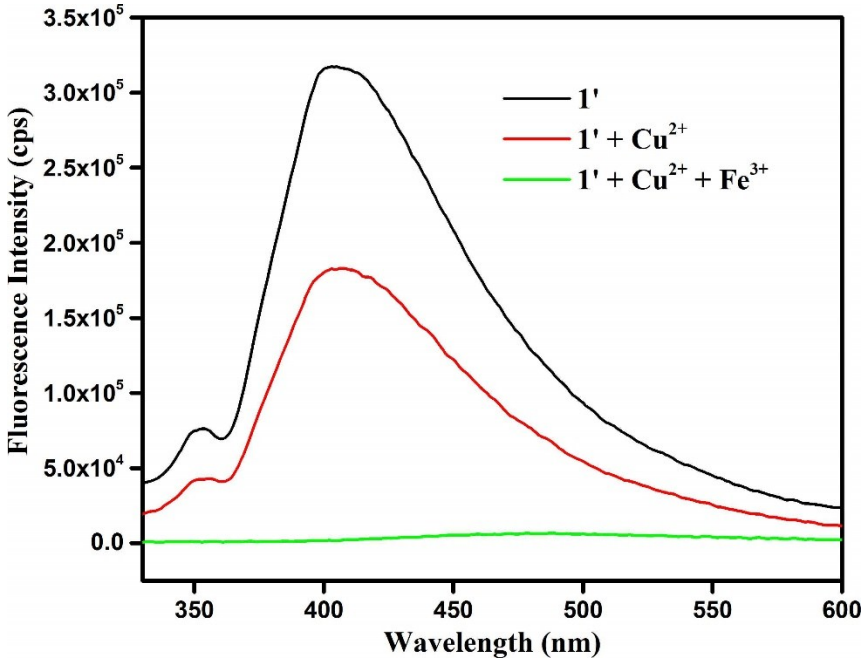

Figure S25. Change in the fluorescence intensity of **1′** upon addition of 10 mM Cu^{2+} solution (400 μL) in presence of 10 mM Fe^{3+} (400 μL) solution.

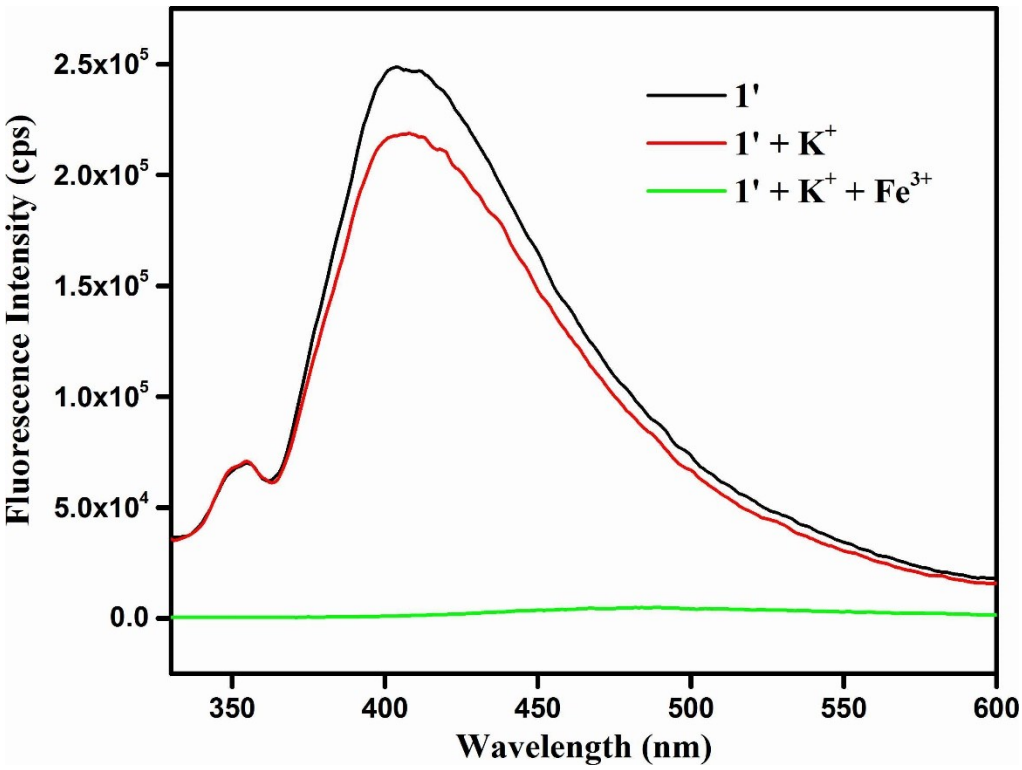

Figure S26. Change in the fluorescence intensity of **1′** upon addition of 10 mM K^{+} solution (400 μL) in presence of 10 mM Fe^{3+} (400 μL) solution.

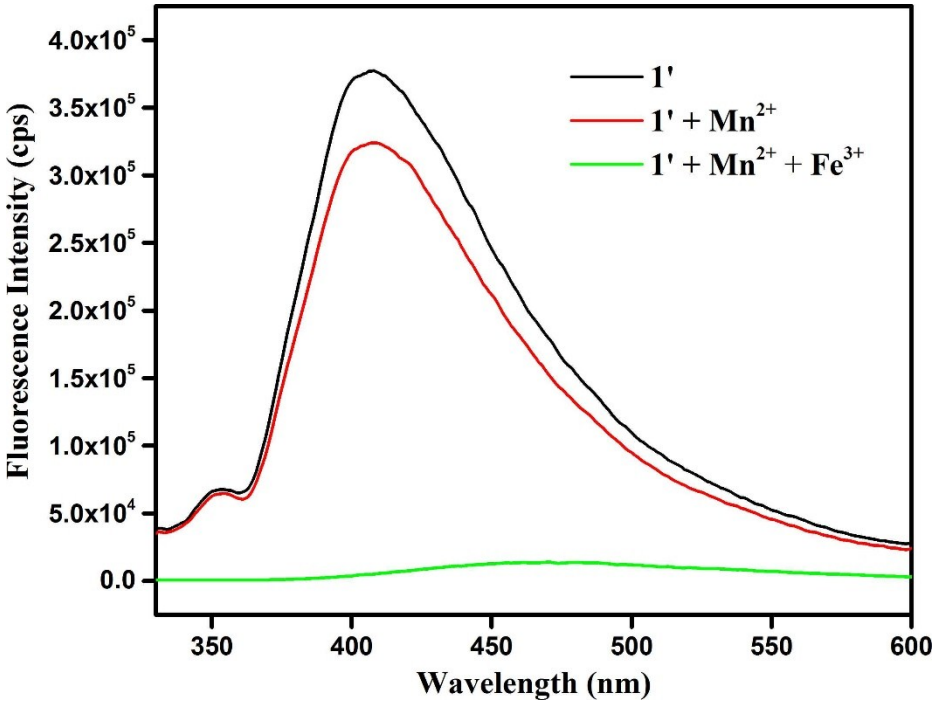

Figure S27. Change in the fluorescence intensity of **1′** upon addition of 10 mM Mn^{2+} solution (400 μL) in presence of 10 mM Fe^{3+} (400 μL) solution.

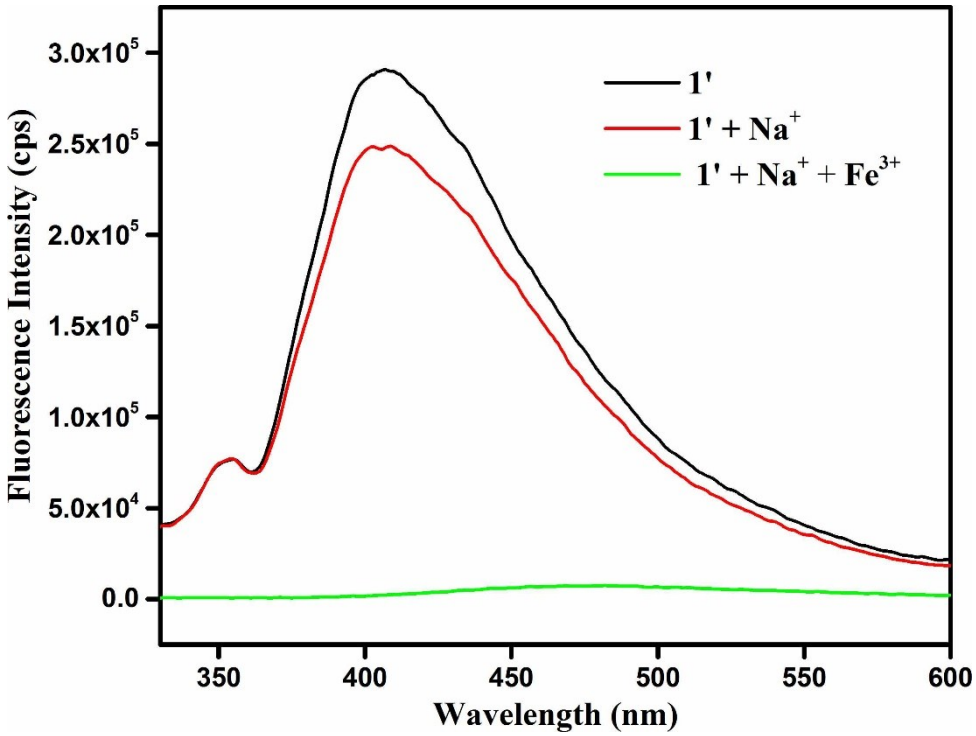

Figure S28. Change in the fluorescence intensity of **1′** upon addition of 10 mM Na^{+} solution (400 μL) in presence of 10 mM Fe^{3+} (400 μL) solution.

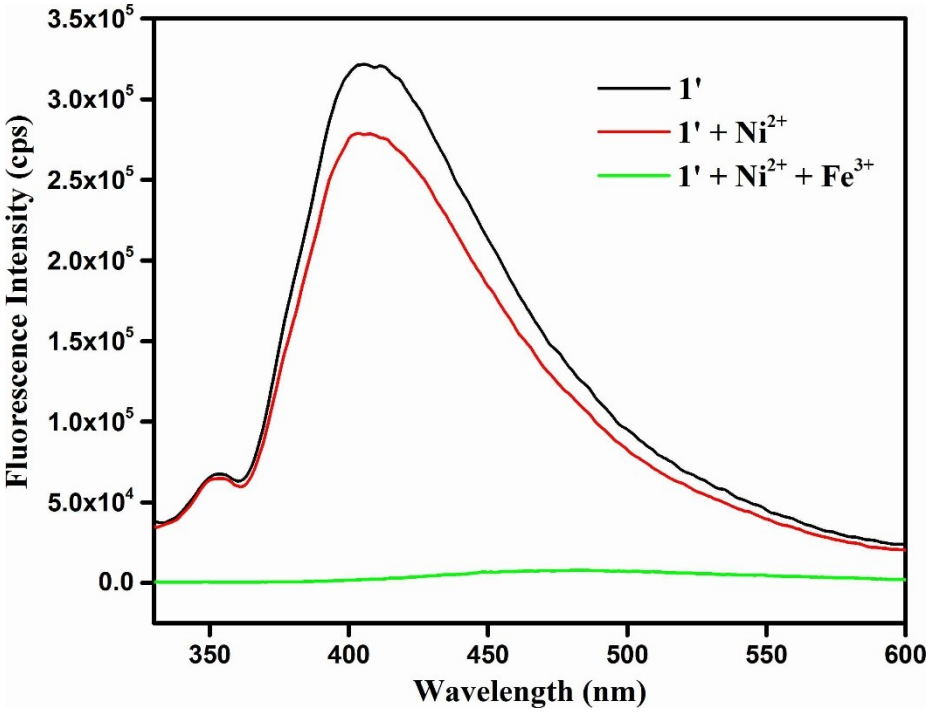

Figure S29. Change in the fluorescence intensity of **1′** upon addition of 10 mM Ni^{2+} solution (400 μL) in presence of 10 mM Fe^{3+} (400 μL) solution.

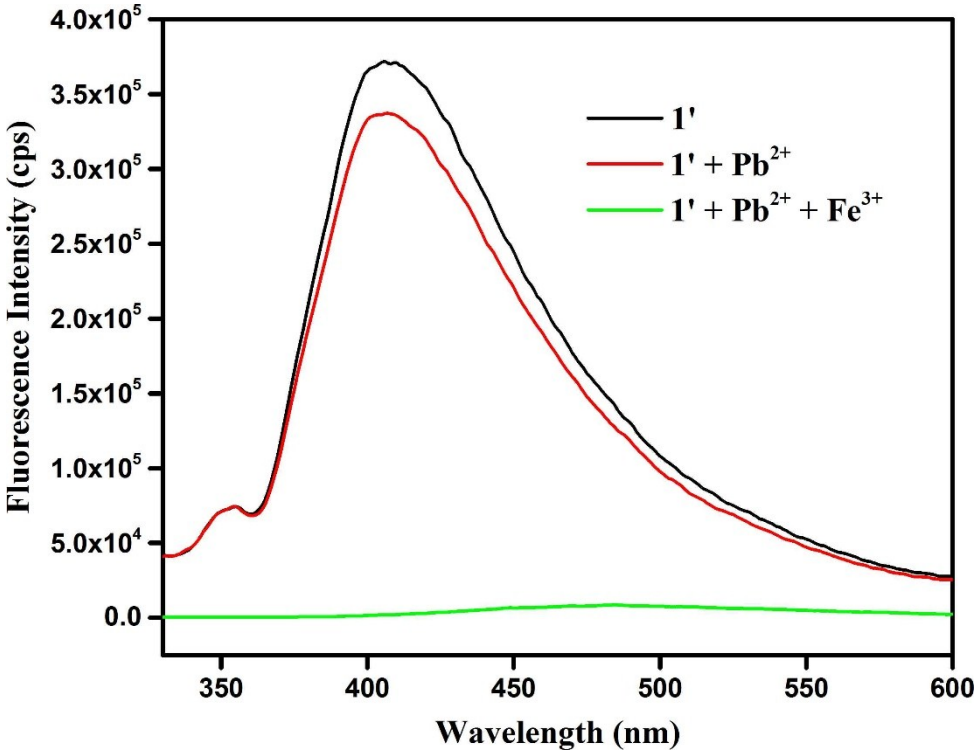

Figure S30. Change in the fluorescence intensity of **1′** upon addition of 10 mM Pb^{2+} solution (400 μL) in presence of 10 mM Fe^{3+} (400 μL) solution.

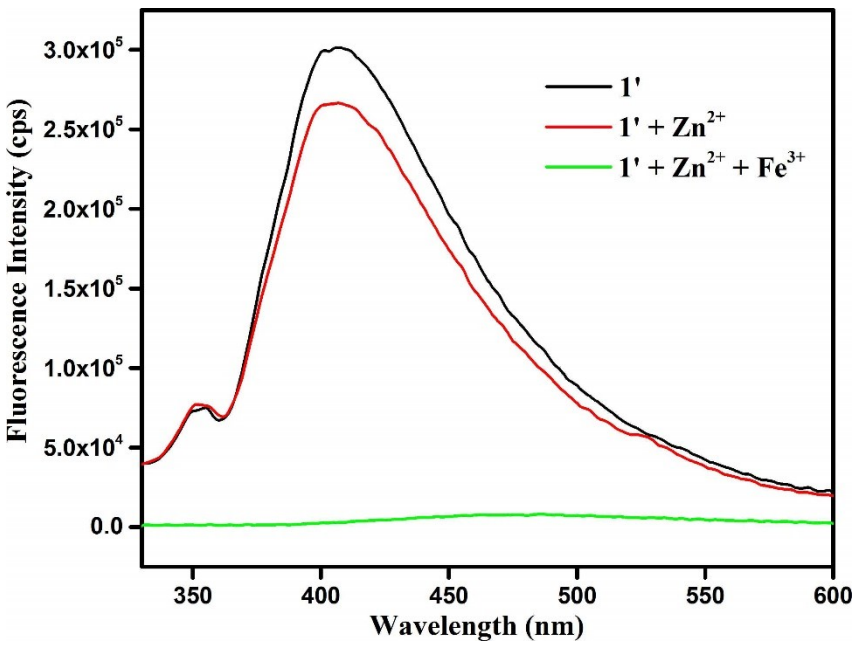

Figure S31. Change in the fluorescence intensity of **1′** upon addition of 10 mM Zn^{2+} solution (400 μL) in presence of 10 mM Fe^{3+} (400 μL) solution.

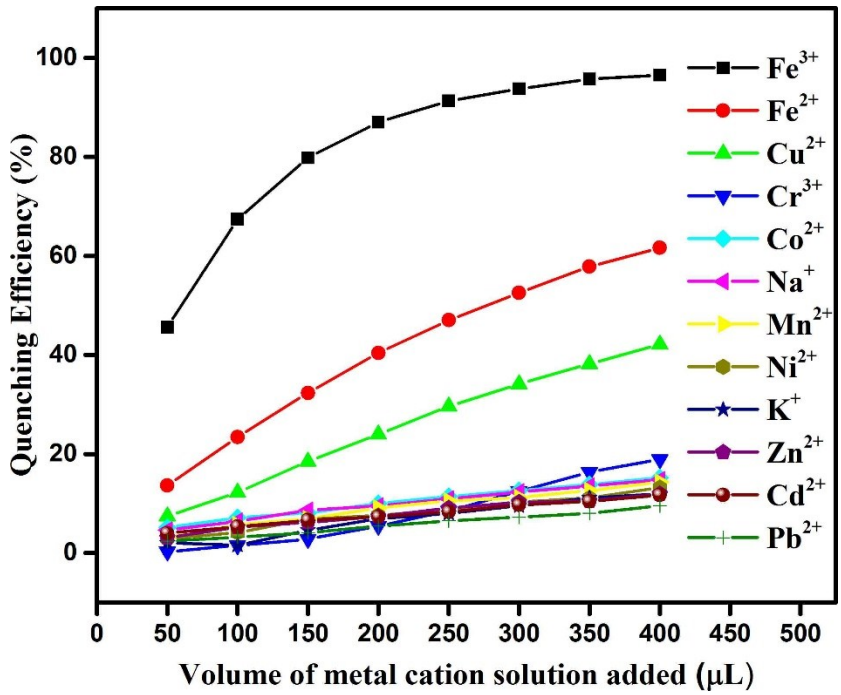

Figure S32. Change of fluorescence quenching efficiencies upon gradual addition of 10 mM solution of various metal cations to a 3 mL well-dispersed suspension of **1′** in methanol.

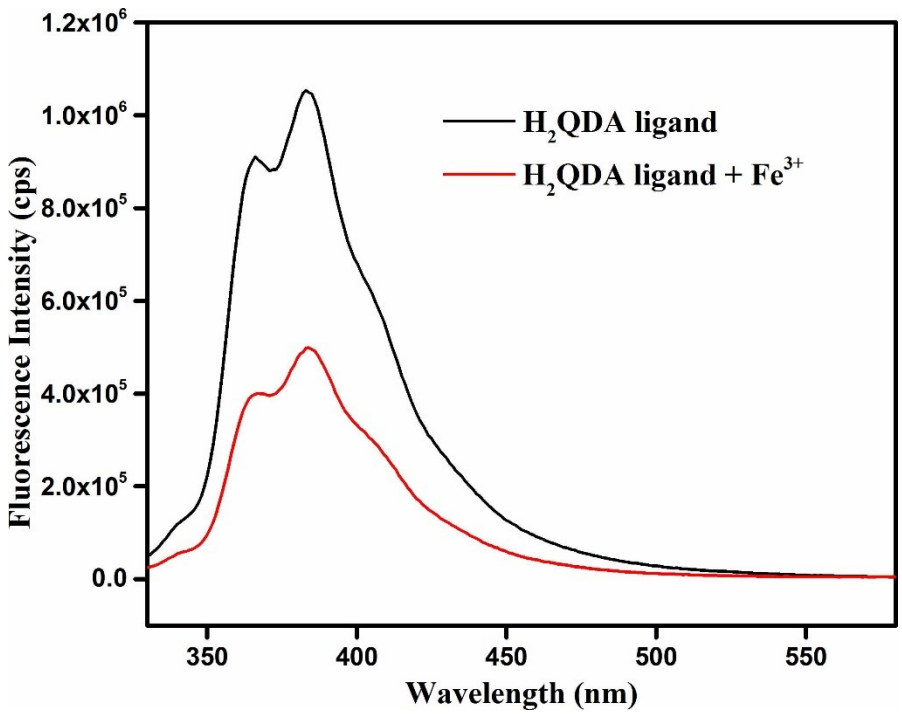

Figure S33. Change in the fluorescence intensity of H_2QDA ligand upon the addition of 400 μL of 10 mM Fe^{3+} solution.

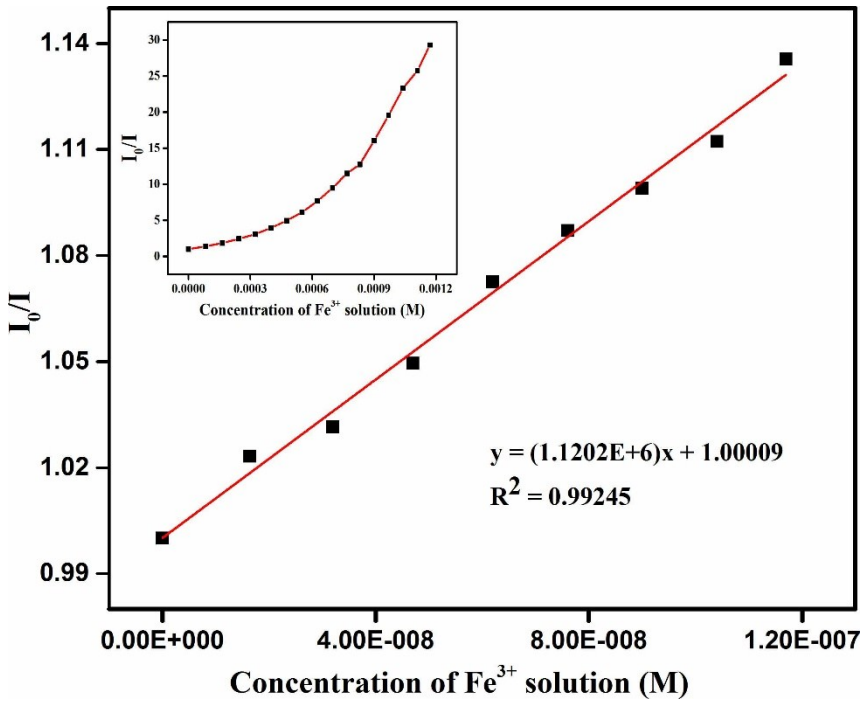

Figure S34. Stern-Volmer plot for the quenching of **1'** at lower concentration of Fe^{3+} solution. Inset: non-linearity of the Stern-Volmer plot at higher concentration of Fe^{3+} solution.

Table S6. A comparison of the Stern-Volmer constant (K_{sv}), detection limit and medium used for the sensing of Fe^{3+} ion for the MOFs reported till date.

Sl. No.	MOF	K_{sv} (M^{-1})	Detection Limit	Medium Used	Ref.
1.	[Zn(QDA)]·0.3DMF	1.12×10^6	2.30×10^{-8} M	methanol	This work
2.	$[La(TPT)(DMSO)_2]\cdot H_2O$	1.36×10^4	-	ethanol	1
3.	$[H(H_2O)_8][DyZn_4(imdc)_4(im)_4]$	2.88×10^4	-	DMSO	2
4.	EuL_3	4.1×10^3	10^{-4} M	ethanol	3
5.	$[Eu_2(MFDA)_2(HCOO)_2(H_2O)_6]\cdot H_2O$	-	3.3×10^{-7} M	DMF	4
6.	$[Cd(H_2L_a)_{0.5}(H_2L_b)_{0.5}(H_2O)]$	-	10^{-5} M	water	5
7.	$[(CH_3)_2NH_2]\cdot[Tb(bptc)]\cdot x$solvents	-	72.76 ppm	ethanol	6
8.	$[Ln_2(Ccbp)_3\cdot 6H_2O]\cdot 3Cl^-\cdot 4H_2O$	1.143×10^5	-	ethanol	7
9.	Eu^{3+}@MIL-124	3.87×10^4	0.28×10^{-6} M	water	8
10.	MIL-53(Al)	-	0.9×10^{-6} M	PBS buffer	9
11.	$[Ln(Hpzbc)_2(NO_3)]\cdot H_2O$	-	2.6×10^{-5} M	ethanol	10
12.	$[Tb(BTB)(DMF)]\cdot 1.5DMF\cdot 2.5H_2O$	-	10^{-5} M	ethanol	11
13.	$[Tb_4(OH)_4(DSOA)_2(H_2O)_8]\cdot(H_2O)_8$	3.5×10^4	-	water	12
14.	Tb^{3+}@Cd-MOF	1.108×10^5	0.010 mM	DMF	13
15.	$[Zr_6O_4(OH)_4(2,7\text{-}CDC)_6]\cdot 19H_2O\cdot 2DMF$	5.5×10^3	9.10×10^{-7} M	water	14
16.	[Cd(*p*-CNPhHIDC)(4,4'-bipy)$_{0.5}$]	1.99×10^3	5×10^{-3} M	water	15
17.	[Zn(*p*-CNPhHIDC)(4,4'-bipy)]	1.37×10^3	5×10^{-3} M	water	15
18.	$[Zr_6O_6(OH)_2(CF_3COO)_2(C_{11}H_5NO_4)_4(H_2O)_4]$	2.25×10^7	1.7×10^{-9} M	water	16
19.	$[Zr_6O_6(OH)_2(CF_3COO)_2(C_{11}H_5NO_4)_4(H_2O)_4]$	1.91×10^7	2.7×10^{-9} M	HEPES buffer	16
20.	$[Al(OH)(BDC\text{-}N_3)]\cdot 1.2H_2O\cdot 0.3DMF$	6.13×10^3	3×10^{-8} M	water	17

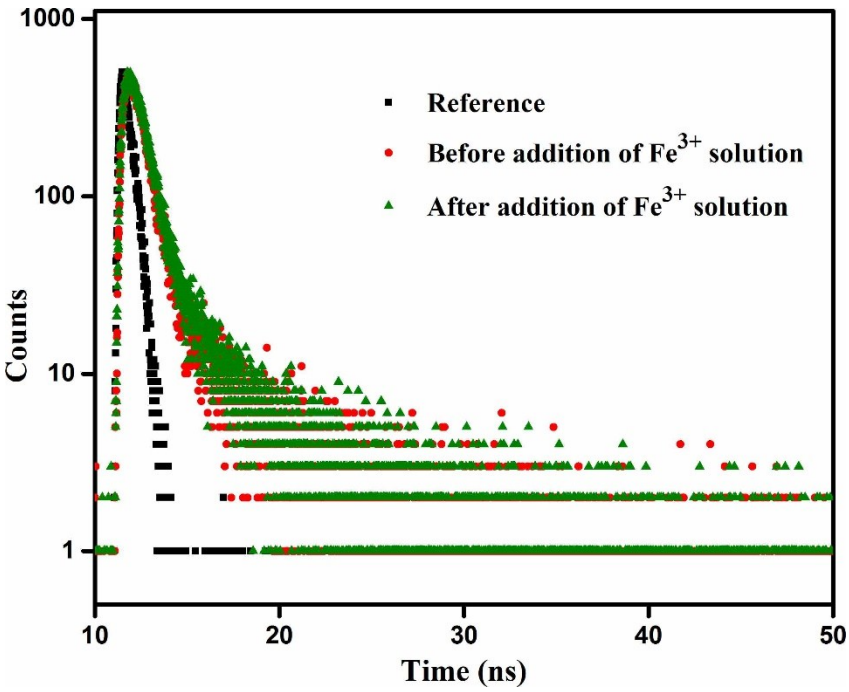

Figure S35. Lifetime decay profile of **1′** before and after addition of 50 μL of 10 mM Fe^{3+} solution.

Table S7. Average excited-state lifetime (<τ>) values of **1'** before and after the addition of 50 μL of 10 mM Fe^{3+} solution (λ_{ex} = 310 nm).

Volume of 10 mM Fe^{3+} solution added (μL)	B_1	B_2	a_1	a_2	τ_1 (ns)	τ_2 (ns)	<τ>* (ns)	χ^2
0	0.038	0.001	0.812	0.188	0.533	3.092	1.014	1.01
50	0.038	0.002	0.793	0.207	0.564	3.040	1.076	1.08

* $\langle\tau\rangle = a_1\tau_1 + a_2\tau_2$

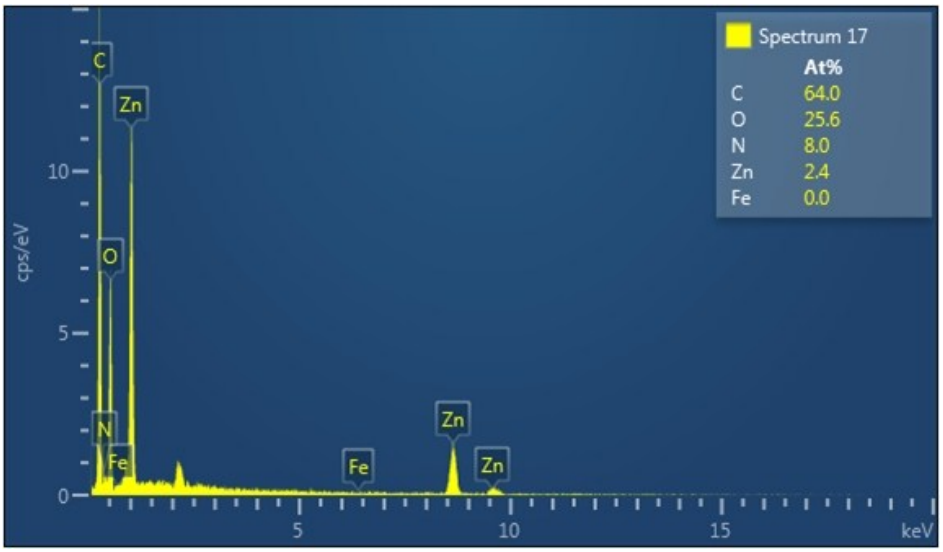

Figure S36. EDX spectrum of **1′** after treatment with 10 mM Fe^{3+} solution.

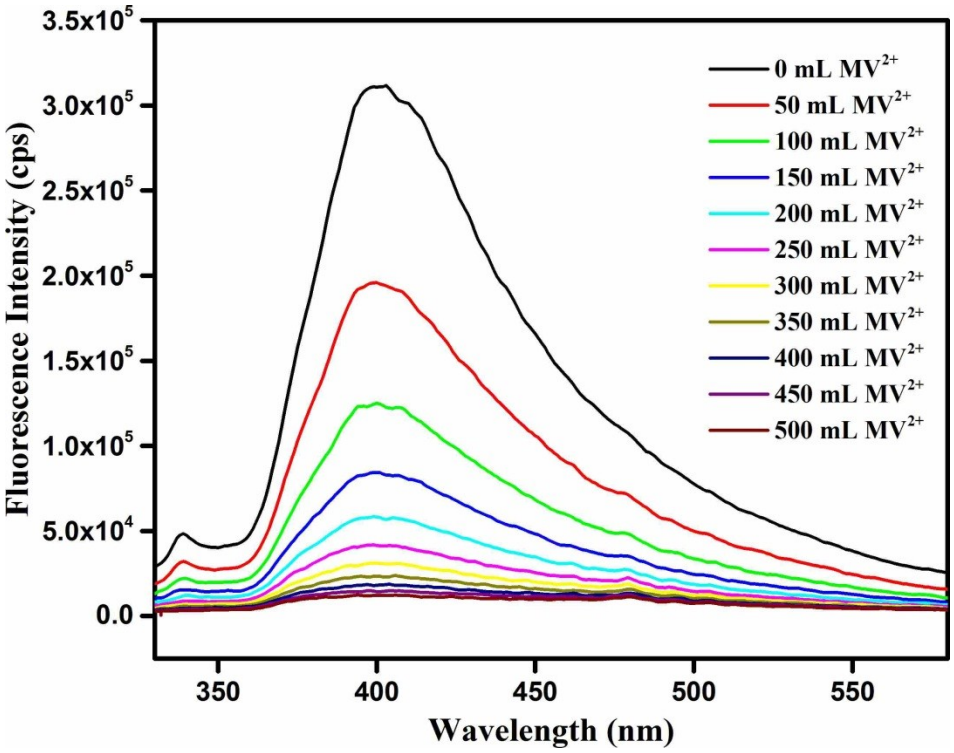

Figure S37. Quenching of the fluorescence intensity of **1′** by incremental addition of 10 mM MV^{2+} solution to a 3 mL stable suspension of **1′** in methanol.

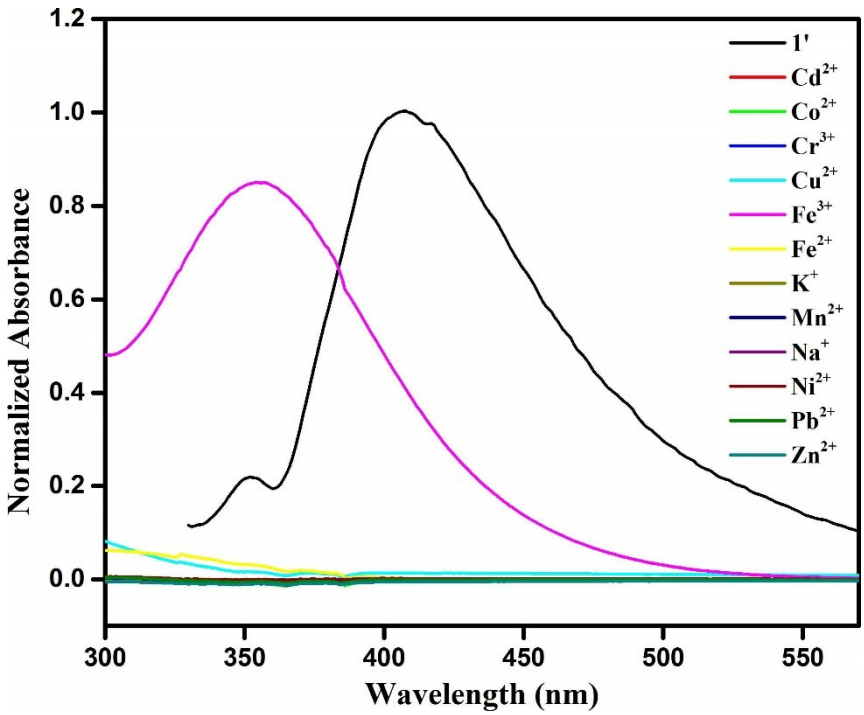

Figure S38. UV-Vis absorption spectra of the different metal ions (10×10^{-3} M) solution in methanol. The emission spectra of **1'** (black color) (3 mg) dispersed in methanol (3 mL).

REFERENCES

1. C. Zhang, Y. Yan, Q. Pan, L. Sun, H. He, Y. Liu, Z. Liang and J. Li, *Dalton Trans.*, 2015, **44**, 13340-13346.
2. Y.-F. Li, D. Wang, Z. Liao, Y. Kang, W.-H. Ding, X.-J. Zheng and L.-P. Jin, *J. Mater. Chem. C*, 2016, **4**, 4211-4217.
3. M. Zheng, H. Tan, Z. Xie, L. Zhang, X. Jing and Z. Sun, *ACS Appl. Mater. Interfaces*, 2013, **5**, 1078-1083.
4. X.-H. Zhou, L. Li, H.-H. Li, A. Li, T. Yanga and W. Huang, *Dalton Trans.*, 2013, **42**, 12403–12409.
5. Y. Wu, G.-P. Yang, Y. Zhang, N. Shi, J. Han and Y.-Y. Wang, *RSC Adv.* , 2015, **5**, 90772-90777.
6. X.-L. Zhao, D. Tian, Q. Gao, H.-W. Sun, J. Xu and X.-H. Bu, *Dalton Trans.*, 2016, **45**, 1040-1046.
7. K.-M. Wang, L. Du, Y.-L. Ma, J.-S. Zhao, Q. Wang, T. Yan and Q.-H. Zhao, *CrystEngComm.*, 2016, **18**, 2690-2700.
8. X.-Y. Xu and B. Yan, *ACS Appl. Mater. Interfaces*, 2015, **7**, 721-729.
9. C.-X. Yang, H.-B. Ren and X.-P. Yan, *Anal. Chem.*, 2013, **85**, 7441−7446.
10. G.-P. Li, G. Liu, Y.-Z. Li, L. Hou, Y.-Y. Wang and Z. Zhu, *Inorg. Chem.*, 2016, **55**, 3952−3959.
11. H. Xu, H.-C. Hu, C.-S. Cao and B. Zhao, *Inorg. Chem.*, 2015, **54**, 4585−4587.
12. X.-Y. Dong, R. Wang, J.-Z. Wang, S.-Q. Wang and T. C. W. Mak, *J. Mater. Chem. A*, 2015, **3**, 641–647.
13. H. Weng and B. Yan, *Sens. Actuator B-Chem.*, 2016, **228**, 702–708.
14. A. Das and S. Biswas, *Sens. Actuator B-Chem.*, 2017, **250**, 121-131.

15. J. Zhang, L. Zhao, Y. Liu, M. Li, G. Li and X. Meng, *New J.Chem.*, 2018, **42**, 6839-6847.
16. C. Gogoi and S. Biswas, *Dalton Trans.*, 2018, *doi: 10.1039/C1038DT03058H*.
17. A. Das, S. Banesh, V. Trivedi and S. Biswas, *Dalton Trans.*, 2018, **47**, 2690-2700.